J Solid State Electrochem (2003) 7: 374–379
DOI 10.1007/s10008-002-0343-y

ORIGINAL PAPER

Seung-Bok Lee · Su-Il Pyun

The kinetics of lithium transport through a composite electrode made of mesocarbon-microbeads heat-treated at 800 °C investigated by current transient analysis

Received: 28 June 2002 / Accepted: 21 October 2002 / Published online: 11 January 2003

Abstract Lithium transport through a mesocarbon-microbeads composite electrode was investigated in a 1 M $LiPF_6$ solution in ethylene carbonate/diethyl carbonate (1:1 by vol%) using a galvanostatic intermittent titration technique and a potentiostatic current transient technique. From analysis of the anodic current transient it is recognized that when the potential step is small enough for the lithium extraction potential to be below the transition potential, the lithium concentration is not fixed at the electrode surface, but the change in surface concentration with time is determined by the ''cell-impedance-controlled'' boundary condition. In contrast, when the potential step is large enough for the lithium extraction potential to be above the transition potential, the ''real potentiostatic'' boundary condition is then established at the electrode surface. Moreover, a ''quasi-current plateau'' was observed in a certain anodic current transient. This experimental result was theoretically analysed, based upon the modified McNabb-Foster equation as a governing equation. This strongly indicates that the difference in activation energies for lithium deintercalation between the different lithium deintercalation sites existing within the electrode accounts for the different kinetics of lithium transport between the different sites.

Keywords Mesocarbon microbeads · Current transient · Lithium transport · McNabb-Foster equation · Cell impedance

S.-B. Lee · S.-I. Pyun (✉)
Department of Materials Science and Engineering,
Korea Advanced Institute of Science and Technology,
373-1 Guseong-Dong Yuseong-Gu, 305-701,
Daejeon, Republic of Korea
E-mail: sipyun@mail.kaist.ac.kr
Tel.: +82-42-8693319
Fax: +82-42-8693310

Introduction

Lithium transport through an electrode made of an intercalation compound has been explored by employing a potentiostatic current transient technique, since this method can be effectively utilized to specify the kinetics of lithium transport through the electrode [1, 2, 3, 4, 5, 6, 7]. Over the last decade, most researches on lithium intercalation have focused on the diffusion of lithium within graphite, assuming that this is the rate-controlling process of the intercalation reaction [8, 9, 10]. However, non-Cottrell behaviour of the plot of the logarithm of the current versus the logarithm of time, with an absolute value of the slope lower than 0.5, has been frequently observed in carbonaceous electrodes [5, 6, 7]. This implies that the lithium concentration which corresponds to the applied potential is not fixed at the electrode surface, but changes with time.

It was reported [11, 12] that some disordered carbons showed higher discharge capacities than the theoretical capacity of graphitic materials. This result strongly indicates that lithium ions are intercalated not only into the graphene layer but also into the extra sites such as the charge-transferring surface site and the cluster gap between the edge planes [11, 12, 13, 14, 15]. Moreover, the potential ranges necessary for lithium intercalation into and deintercalation from the graphene layer and extra sites are different among themselves, which is caused by the difference in activation energies for lithium intercalation into and deintercalation from the respective sites [14, 16, 17, 18, 19].

This work is aimed first at establishing the boundary condition for lithium transport at the mesocarbon-microbeads (MCMB) electrode surface, and then at elucidating the mechanism of lithium transport through the MCMB electrode, which contains different kinds of lithium deintercalation sites. For this purpose, open-circuit potential transients and potentiostatic current transients were first experimentally measured. Next, we numerically simulated the anodic current transients

based upon the modified McNabb-Foster equation as a governing equation in combination with the "cell-impedance-controlled" constraint as a boundary condition, to compare with the transient experimentally measured.

Experimental

Green MCMB (Osaka Gas) powder was heat-treated at 800 °C for 3 h under an argon stream with a flow rate of 500 cm^3/min (standard cubic centimeters per minute). The heat-treated MCMB electrode specimen was prepared by mixing the MCMB powder with 10 wt% poly(vinylidene fluoride) (PVDF) as a binder in *N*-methylpyrrolidone (NMP) solution, followed by pasting on Cu foil and drying in a vacuum oven at 110 °C for 8 h. A three-electrode electrochemical cell was employed for the electrochemical measurements. The PVDF-bonded MCMB composite electrode was used as the working electrode with an apparent (exposed) area of 1 cm^2. The reference and counter electrodes were constructed from pure lithium foil (Foote Mineral, USA; purity 99.9%), and 1 M $LiPF_6$ in ethylene carbonate/diethyl carbonate (EC/DEC) (50:50 by vol%) solution was used as the electrolyte.

For electrochemical measurements, a Solartron 1255 Frequency Response Analyzer (FRA) was used in conjunction with a Solartron 1287 Electrochemical Interface (ECI). Galvanostatic intermittent discharge experiments were conducted under the condition that the discharge current was selected so that a change in lithium content of $\Delta\delta = 1$ for $Li_\delta C_6$ would occur for 5 h. The anodic current transient was measured on the electrode by jumping from the initial potentials of 0.30 and 1.10 $V_{Li/Li+}$ to various lithium extraction potentials, E_{ext}. Prior to lithium deintercalation, the electrode was maintained at the initial potential for a sufficiently long time to obtain a low steady-state current. The electrochemical impedance measurements were carried out by applying an a.c. amplitude of 5 mV_{RMS} on an electrode potential, E, of 0.30 $V_{Li/Li+}$ over the frequency range from 5×10^{-2} to 10^5 Hz. All the electrochemical experiments were performed in a glove box (Mecaplex GB94) filled with purified argon gas.

Results and discussion

Figure 1 presents the electrode potential E obtained from the galvanostatic intermittent discharge curve measured on the PVDF-bonded MCMB composite electrode in 1 M $LiPF_6$-EC/DEC solution as a function of intercalated lithium content. The electrode potential curve did not show any "potential plateaux"; rather, it ran continuously throughout the whole lithium deintercalation. This means that the MCMB heat-treated at 800 °C still has a very low degree of crystallinity, and hence lithium is deintercalated from the MCMB particles without formation of any thermodynamically stable phases.

It was reported [14, 16, 17, 18, 19] that there exist four kinds of lithium deintercalation sites within soft carbon heat-treated at low temperature, such as a charge-transferring surface site, an intercalation site between graphene layers, a zigzag site in the edge plane and, finally, an armchair site in the edge plane, which are designated as the sites for Type I, Type II, Type III-1 and Type III-2, respectively. In addition, the potential necessary for lithium deintercalation from the sites for Type I, Type II, Type III-1 and Type III-2 ranges between 0.25 and 1.5 $V_{Li/Li+}$, 0 and 0.25 $V_{Li/Li+}$, 0 and 0.10 $V_{Li/Li+}$ and 0.10 and 0.40 $V_{Li/Li+}$, respectively. The potential ranges necessary for lithium deintercalation from the four different lithium deintercalation sites within the MCMB are also given in Fig. 1.

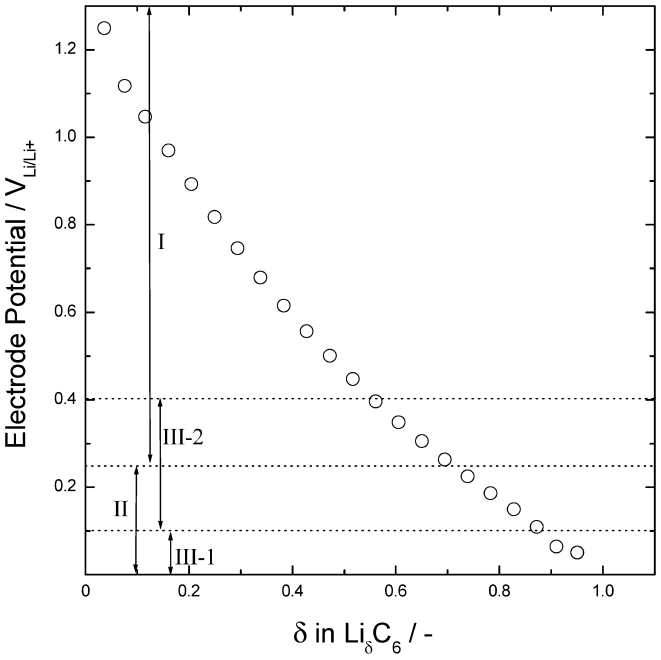

Fig. 1 The galvanostatic intermittent discharge curve measured on the PVDF-bonded MCMB composite electrode in 1 M $LiPF_6$-EC/DEC solution. The MCMB powder was previously heat-treated at 800 °C. Regions I, II, III-1 and III-2 represent the potential ranges necessary for lithium deintercalation from the sites for Type I, Type II, Type III-1 and Type III-2, respectively

Figure 2 illustrates on a logarithmic scale the anodic current transient experimentally measured on the electrode in 1 M $LiPF_6$-EC/DEC solution by jumping from the initial electrode potential, $E = 1.10$ $V_{Li/Li+}$, to various lithium extraction potentials, $E_{ext} = 1.15$–1.55 $V_{Li/Li+}$. In the lithium extraction potential E_{ext} higher than 1.30 $V_{Li/Li+}$, the anodic current transient clearly exhibits a linear relationship between the logarithm of the current and the logarithm of time, with a slope of 0.5, representing Cottrell behaviour, followed by an exponential decay with time. Moreover, the current transients clearly share shape and value with one another, since the concentration of lithium transferred during the potential jumps, c_{Li}, has an almost constant value of 2.0×10^{-3} mol cm^{-3}, regardless of the value of E_{ext}. This means that the "real potentiostatic" boundary condition is established at the electrode surface at E_{ext} above 1.30 $V_{Li/Li+}$.

However, in the lithium extraction potential with E_{ext} lower than 1.30 $V_{Li/Li+}$, the logarithmic current transient shows a linear relationship between the logarithm of the current and the logarithm of time, with a slope between −0.5 and 0, followed by an exponential decay with time. As E_{ext} increases up to 1.30 $V_{Li/Li+}$, the slope of the logarithmic current transient decreases down to –0.5.

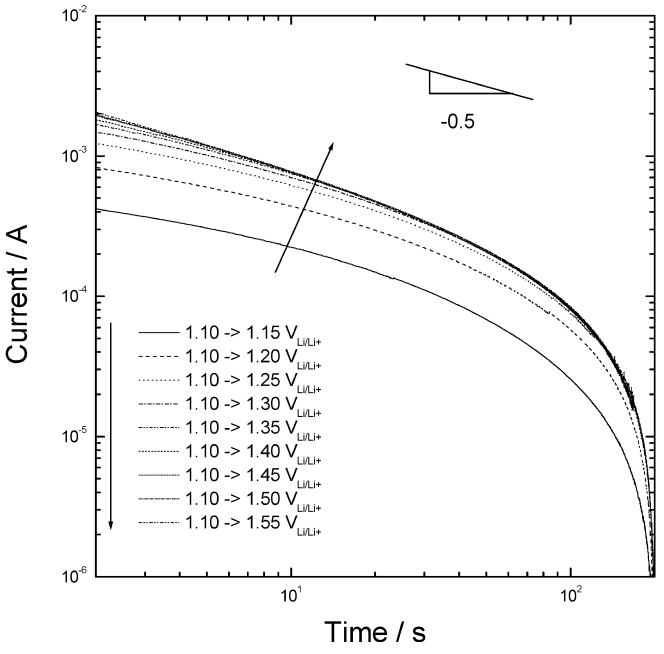

Fig. 2 The anodic current transient experimentally obtained from the PVDF-bonded MCMB composite electrode in 1 M $LiPF_6$-EC/DEC solution at potential jumps from 1.10 $V_{Li/Li+}$ to various lithium extraction potentials as indicated on the figure. The MCMB powder was previously heat-treated at 800 °C

In order to more clearly specify the boundary condition for lithium transport, the initial current level, i_{ini}, at 5 s was calculated under the "real potentiostatic" boundary condition as well as under the "cell-impedance-controlled" boundary condition. It should be noted that in order to disregard the double layer discharging effect [20], the value of i_{ini} calculated at 5 s was considered.

First, the value of i_{ini} was calculated under the "real potentiostatic" boundary condition from the analytical solution of the diffusion equation in the short time region in the case of spherical electrodes [1] as follows:

$$i(t) = \frac{zFc_{Li}A_{ea}\sqrt{\tilde{D}_{Li}}}{\sqrt{\pi t}} + \frac{zFc_{Li}A_{ea}\tilde{D}_{Li}}{R*} \quad (1)$$

Here, z is the valence number of the lithium ion, F the Faraday constant, A_{ea} the electrochemically active area, $\tilde{D}_{Li}$ the chemical diffusivity of lithium, t the deintercalation time, and $R*$ represents the average radius of the MCMB particle. In this work we call Eq. 1 the modified Cottrell equation. By taking the values of the parameters c_{Li}, A_{ea}, $\tilde{D}_{Li}$ and $R*$ as 2.0×10^{-3} mol cm^{-3}, 1.56 cm^2, 2×10^{-10} cm^2 s^{-1} and 5 μm, respectively, we calculated the value of i_{ini} at 5 s from the modified Cottrell equation.

It should be stressed that the current transient of Fig. 2 was measured at the potential jump from a high initial electrode potential E, for example 1.10 $V_{Li/Li+}$, that corresponds to a very low equilibrium concentration, c, of lithium in the electrode to a higher lithium extraction potential, E_{ext}, that corresponds to $c\approx0$ in the electrode, regardless of E_{ext}. Hence the value of i_{ini} was calculated under the "real potentiostatic" boundary condition from the modified Cottrell equation to be a very small constant value. The calculated values are plotted against E_{ext} in Fig. 3 as open circles.

Next, the value of i_{ini} was calculated under the "cell-impedance-controlled" boundary condition from Ohm's law as follows:

$$i(t) = zFA_{ea}\tilde{D}_{Li}\left|\frac{\partial c}{\partial r}\right| = \frac{\Delta E(t)}{R_{cell}} \quad (2)$$

Here, c is the equilibrium concentration of lithium, r the distance from the centre of the particle, $\Delta E(t) = |E_{ext} - E|$, the potential difference between the lithium extraction potential E_{ext} and the initial electrode potential E, and R_{cell} represents "cell impedance". We calculated the value of i_{ini} at 5 s, by taking the value of R_{cell} at the electrode potential E of 1.10 $V_{Li/Li+}$ as 173 Ω. The calculated values are also shown as a function of E_{ext} in Fig. 3 (denoted by open triangles). The value of i_{ini} calculated under the "cell-impedance-controlled" boundary condition is linearly proportional to the value of E_{ext}. In this work, we can define the transition potential E_{tr} as the potential at which the plot of i_{ini} versus E_{ext} calculated by the modified Cottrell equation intersects the plot calculated from Ohm's law. The value of E_{tr} was determined to be ca. 1.30 $V_{Li/Li+}$ from Fig. 3.

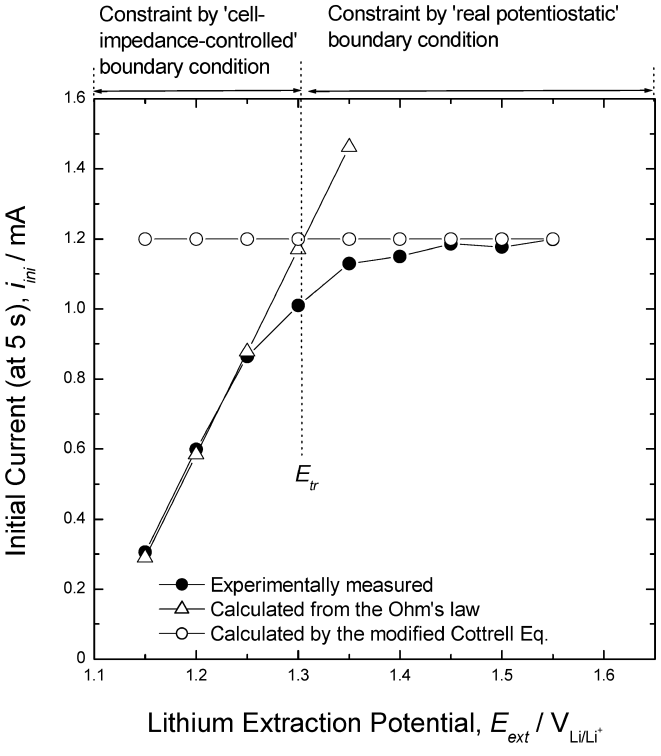

Fig. 3 Plot of the initial current level i_{ini} against the lithium extraction potential, E_{ext}. *Filled circles*: experimentally measured from the current transient of Fig. 2; *open triangles*: calculated from Ohm's law; *open circles*: calculated by the modified Cottrell equation

For comparison between the measured and the calculated values of i_{ini}, the value of i_{ini} measured at 5 s (filled circles) is plotted along with the two kinds of calculated values (open circles, open triangles) in Fig. 3. As discussed in [20], the double layer discharging is already finished at the moment $t = 5$ s. In Fig. 3, the measured value is almost identical to the value calculated from the modified Cottrell equation above the transition potential, E_{tr}, of 1.30 $V_{Li/Li+}$, which means that the "real potentiostatic" boundary condition is established at the electrode surface. On the other hand, the measured value coincides fairly well with the value calculated from Ohm's law below $E_{tr} = 1.30$ $V_{Li/Li+}$, which means that the "cell-impedance-controlled" boundary condition is satisfied at the electrode surface.

Now we can assert that the boundary condition for lithium transport at the electrode surface changes from the "cell-impedance-controlled" boundary condition to the "real potentiostatic" boundary condition as E_{ext} increases. Similarly, we have already reported that the boundary condition for hydrogen transport at the Pd electrode surface changes from the constraint of "Butler-Volmer behaviour" to the "real potentiostatic" boundary condition with increasing hydrogen discharging potential [21]. It is concluded that the "real potentiostatic" boundary condition is always satisfied at such an electrode/electrolyte interface, when an extraction potential is subjected to that interface high enough so that the diffusion flux of lithium and hydrogen is just exceeded by the "cell-impedance-controlled" flux of lithium or the charge transfer flux of hydrogen. Even though lithium transport through carbon and hydrogen transport through Pd or metal hydrides proceed by different mechanisms, the above assertion is valid for lithium transport as well as for hydrogen transport in a similar manner.

Figure 4 gives on a logarithmic scale the anodic current transient experimentally obtained from the PVDF-bonded MCMB composite electrode in 1 M $LiPF_6$-EC/DEC solution. The anodic current transient was measured at the potential jump from 0.30 $V_{Li/Li+}$ to the lithium extraction potentials, E_{ext}, of 0.32–0.42 $V_{Li/Li+}$.

It is worth noting that in this case the value of c_{Li} is so large that the value of i_{ini} calculated under the "real potentiostatic" boundary condition from the modified Cottrell equation is always larger than that of i_{ini} calculated under the "cell-impedance-controlled" boundary condition from Ohm's law. Thus, the value of i_{ini} experimentally measured at 5.0 s from the current transient of Fig. 4 was smaller than that of i_{ini} theoretically calculated from the modified Cottrell equation (Eq. 1) [1]. One value of i_{ini} calculated from the modified Cottrell equation at the potential jump from 0.30 to 0.34 $V_{Li/Li+}$ is representatively shown in Fig. 4. Moreover, all the current transients did not follow the Cottrell behaviour, which means a linear relationship between log i and log t with a slope of –0.5, but they obeyed Ohm's law.

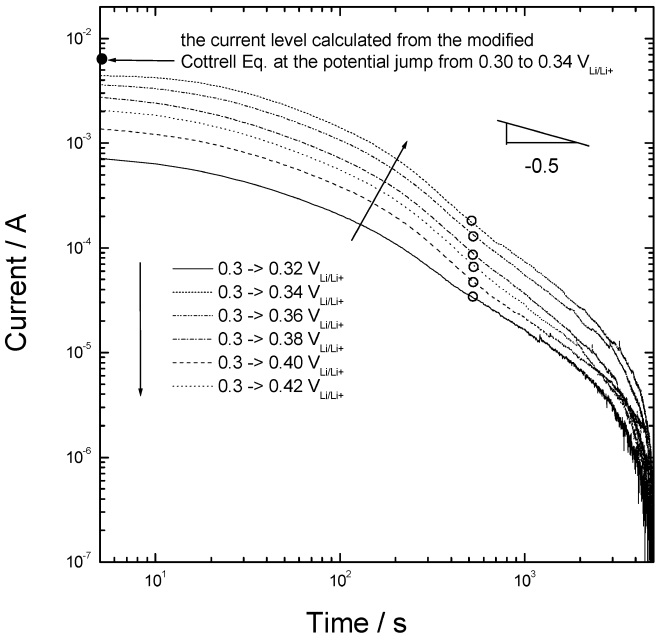

Fig. 4 The anodic current transient experimentally obtained from the PVDF-bonded MCMB composite electrode in 1 M $LiPF_6$-EC/DEC solution at potential jumps from 0.30 $V_{Li/Li+}$ to various lithium extraction potentials as indicated on the figure. The MCMB powder was previously heat-treated at 800 °C

In addition, it is noted that the value of "cell impedance" (27.8 Ω) at the electrode potential, E, of 0.30 $V_{Li/Li+}$, calculated from the slope of i_{ini} versus ΔE, coincided well with the internal cell resistance (28.2 Ω) obtained from a.c. impedance spectra measured on the PVDF-bonded MCMB composite electrode. Based upon the linear relationship between i_{ini} and ΔE, and the coincidence in value between "cell impedance" and the internal cell resistance, it is strongly suggested that lithium transport through the PVDF-bonded MCMB composite electrode proceeds under the "cell-impedance-controlled" constraint at the potential jumps from 0.30 $V_{Li/Li+}$ to the lithium extraction potentials from 0.32 to 0.42 $V_{Li/Li+}$. This means that no transition of the "cell-impedance-controlled" boundary condition occurs in the E_{ext} range 0.32–0.42 $V_{Li/Li+}$.

The shape of the current transient measured at the potential jump from 0.30 $V_{Li/Li+}$ (Fig. 4) was somewhat different from that measured at the potential jump from 1.10 $V_{Li/Li+}$ (Fig. 2). The former current transient showed three-stage current transient behaviour, which is characterized by the presence of an inflexion point or a "quasi-current plateau". In contrast, the latter current transient showed two-stage current transient behaviour, i.e. a monotonic decrease in logarithmic current with logarithmic time, followed by the exponential decay, which represents simple diffusion of lithium through a single microcrystalline phase.

Remembering the potential range for lithium deintercalation, it should be noted that lithium ions present

in the site for Type I can be deintercalated only by the potential jump from 1.10 $V_{Li/Li+}$ to E_{ext} ranging from 1.15 to 1.55 $V_{Li/Li+}$. In contrast, lithium ions residing in the site for Type III-2, as well as the site for Type I, can be deintercalated by potential jumps from 0.30 $V_{Li/Li+}$ to E_{ext} in the range 0.32–0.42 $V_{Li/Li+}$.

It is well known [20] that under the "cell-impedance-controlled" constraint the presence of an inflexion point or "current plateau" in the current transient is due to the presence of a "potential plateau", indicating the coexistence of two phases in the electrode potential curve. However, the anodic current transient measured at the potential jump from 0.30 $V_{Li/Li+}$ (Fig. 4), at which both lithium ions residing at the sites for Type I and Type III-2 can be deintercalated during the potential jump, clearly showed an inflexion point or a "current plateau" even though the electrode potential curve did not show any "potential plateau" throughout the whole lithium deintercalation. In this work, such abnormal current transient behaviour showing an "inflexion point" at the potential jump from 0.30 $V_{Li/Li+}$ could be reasonably explained in terms of the difference in activation energies for lithium deintercalation.

Now, let us theoretically model the current transient showing an inflection point or a "quasi-current plateau" measured on the PVDF-bonded MCMB composite electrode. Since lithium transport through the different kinds of lithium deintercalation sites present within the MCMB is conceptually similar to hydrogen transport through the normal sites and the trap sites existing within metal, the McNabb-Foster equation [5, 6, 7, 22, 23] holds for the case of lithium transport through the MCMB. In addition, since the MCMB contains three-dimensional diffusion paths and the individual particle is observed to be almost spherical in shape, we selected the constituent particle of spherical symmetry for theoretical calculation.

Thus, in this work, the McNabb-Foster equation was modified to satisfy spherical symmetry and it was used as a governing equation for lithium transport as follows:

$$\tilde{D}_{Li}\left[\frac{2}{R^*}\left(\frac{\partial c}{\partial r}\right)+\frac{\partial^2 c}{\partial r^2}\right]=\frac{\partial c}{\partial t}+N\frac{\partial \theta}{\partial t} \tag{3}$$

with the rate of reversible trapping into and escaping from the trap sites described by:

$$\frac{\partial \theta}{\partial t}=kc(1-\theta)-p\theta \tag{4}$$

where N is the concentration of the trap sites, θ the fraction of the trap sites occupied, k the capture rate into the trap sites, and p represents the release rate from the trap sites. The initial condition (IC) and the boundary conditions (BC) are given as:

$$\text{IC}: \quad c=c_0 \text{ for } 0<r<R^* \text{ at } t=0 \tag{5}$$

$$\text{BC}: \quad zFA_{ea}\tilde{D}_{Li}\left(\frac{\partial c}{\partial r}\right)=0 \text{ (impermeable constraint)} \tag{6}$$

for $r=0$ at $t\geq 0$ and:

$$\text{BC}: \quad zFA_{ea}\tilde{D}_{Li}\left|\frac{\partial c}{\partial r}\right| = \frac{\Delta E}{R_{cell}} \text{ (“cell} - \text{impedance} - \text{controlled”) constraint} \tag{7}$$

for $r=R^*$ at $t>0$.

The capture rate (k) and release rate (p) are defined as the number of lithium jumps per unit time from the lattice site to the trap site and jumps that per unit time from the trap site to the lattice site, respectively. From the Arrhenius plot of $\tilde{D}_{Li}$, the activation energies for lithium deintercalation from the sites for Type I and Type III-2 were calculated to be 87.23 kJ mol^{-1} and 78.51 kJ mol^{-1}, respectively, and then the values of k and p were determined to be 2.88×10^{-2} s^{-1} and 8.53×10^{-4} s^{-1}, respectively.

At the same time, from the analysis of the galvanostatic intermittent discharge curve measured on the PVDF-bonded MCMB composite electrode, the concentration of the site for Type I, N, was determined to be 1.4×10^{-2} mol cm^{-3} and the fractions of the lithium occupied at the site for Type I were found to be 0.999, 0.998, 0.995, 0.990, 0.980 and 0.957 at E_{ext} values of 0.32, 0.34, 0.36, 0.38, 0.40 and 0.42 $V_{Li/Li+}$, respectively.

Figure 5 illustrates on a logarithmic scale the anodic current transient under the electrode potential jumps from 0.30 $V_{Li/Li+}$ to various lithium extraction potentials, E_{ext}, of 0.32–0.44 $V_{Li/Li+}$, determined from the numerical solution to the modified McNabb-Foster

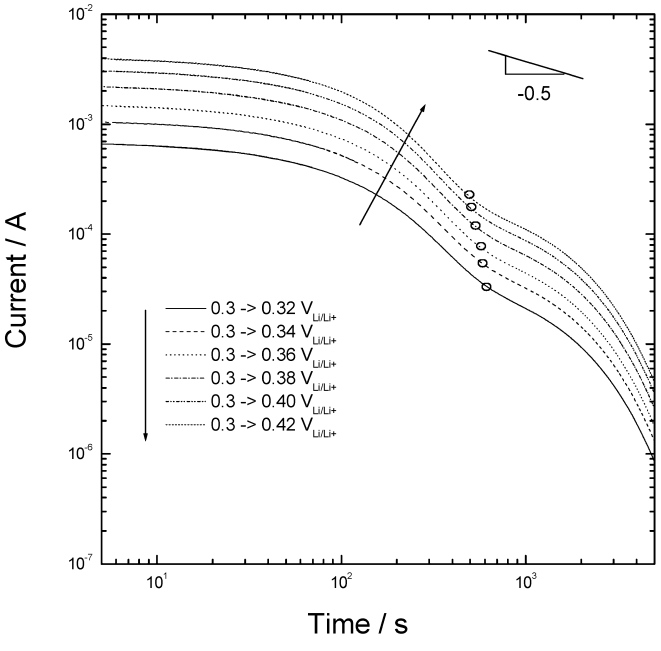

Fig. 5 The anodic current transient theoretically calculated based upon the modified McNabb-Foster equation at potential jumps from 0.30 $V_{Li/Li+}$ to various lithium extraction potentials under the "cell-impedance-controlled" constraint, by taking $A_{ea}=1.56$ cm^2, $\tilde{D}_{Li}=2\times10^{-10}$ cm^2 s^{-1}, $R_{cell}=27.8$ Ω and $R^*=5$ μm

equation of Eqs. 3 and 4 with IC and BC of Eqs. 5, 6, 7 by taking the values described above. The anodic current transient at the potential jump from 0.30 to various lithium extraction potentials clearly showed the three-stage current transient behaviour which is characterized by an inflexion point or a ''quasi-current plateau''.

The anodic current transient theoretically calculated based upon the modified McNabb-Foster equation along with the ''cell-impedance-controlled'' constraint of Fig. 5 almost coincided with the current transient experimentally measured of Fig. 4 in value and in shape. This strongly indicates that the appearance of an inflexion point in the current transient is due to lithium deintercalation from two different kinds of deintercalation sites with clearly distinguishable activation energies.

Conclusion

In the present work, the mechanism of lithium transport through the PVDF-bonded MCMB composite electrode has been investigated by means of analysis of the anodic current transient. The results are summarized as follows:

1. When the electrode surface is subjected to a constant lithium extraction potential, E_{ext}, the lithium concentration gradient at the electrode surface is specified by the ''cell-impedance-controlled'' boundary condition below the transition potential, E_{tr}, whereas the constraint of the ''real potentiostatic'' boundary condition is satisfied at the electrode surface above E_{tr}.
2. The difference in activation energies for lithium deintercalation between the different lithium deintercalation sites existing within the MCMB composite electrode is responsible for the different kinetics of lithium transport through the different lithium deintercalation sites, which leads to the presence of the inflexion point or ''quasi-current plateau'' in the current transient.

Acknowledgements The receipt of a research grant under the internal research programme ''Technological Development of High Performance Lithium Battery'' from the Korea Advanced Institute of Science and Technology (KAIST), 2000/2002, is gratefully acknowledged. This work was also partly supported by the Brain Korea 21 project.

References

1. Macdonald DD (1977) Transient techniques in electrochemistry. Plenum Press, New York, p 69
2. Wen CJ, Boukamp BA, Huggins RA, Weppner W (1979) J Electrochem Soc 126:2258
3. Shin HC, Pyun SI (1999) Electrochim Acta 45:489
4. Pyun SI, Kim SW (2001) J Power Sources 97/98:371
5. Pyun SI, Lee SB, Chang WY (2002) J New Mater Electrochem Syst 5:281
6. Chang WY, Pyun SI, Lee SB (2002) J Solid State Electrochem (in press)
7. Lee SB, Pyun SI (2002) Electrochim Acta 48:419
8. Funabiki A, Inaba M, Abe T, Ogumi Z (1999) J Electrochem Soc 146:2443
9. Wang C, Kakwan I, Appleby AJ, Little FE (2000) J Electroanal Chem 489:55
10. Shimizu A, Tachikawa H (2002) J Phys Chem Solids 63:619
11. Sato K, Noguchi M, Demachi A, Oki N, Endo M (1994) Science 264:556
12. Yata S, Kinoshita H, Komori M, Ando N, Kashiwamura T, Harada T, Tanaka K, Yamabe T (1994) Synth Met 62:153
13. Liu YH, Xue JS, Zheng T, Dahn JR (1996) Carbon 34:193
14. Mochida I, Ku CH, Korai Y (2001) Carbon 39:399
15. Gerald RE, Sanchez J, Johnson CS, Klingler RJ, Rathke JW (2002) J Phys Condens Matter 13:8269
16. Boehm RC, Banerjee A (1992) J Chem Phys 96:1150
17. Marquez A, Vargas A, Balbuena PB (1998) J Electrochem Soc 145:3328
18. Ago H, Kato M, Yahara K, Yoshizawa K, Tanaka K, Yamabe T (1999) J Electrochem Soc 146:1262
19. Gong J, Wu H (2000) Electrochim Acta 45:1753
20. Shin HC, Pyun SI (2002) In: White RE, Conway BE, Vayenas CG (eds) Modern aspects of electrochemistry, vol 36. Plenum Press, New York, pp 255–301
21. Han JN, Seo M, Pyun SI (2001) J Electroanal Chem 499:152
22. McNabb A, Foster PK (1963) Trans Met Soc AIME 227:618
23. Pyun SI, Yang TH (1998) J Electroanal Chem 441:183